International Journal of Chemical, Materials and Biomolecular Sciences
ISSN: 2415-6620
Vol:6, No:8, 2012

The Importance of 3D Mesh Generation for Large Eddy Simulation of Gas – Solid Turbulent Flows in a Fluidized Beds

G. González-Silva, E. M. Matos, W. P. Martignoni, M. Mori

***Abstract*—**The objective of this work is to show a procedure for mesh generation in a fluidized bed using large eddy simulations (LES) of a filtered two-fluid model. The experimental data were obtained by [1] in a laboratory fluidized bed. Results show that it is possible to use mesh with less cells as compared to RANS turbulence model with granular kinetic theory flow (KTGF). Also, the numerical results validate the experimental data near wall of the bed, which cannot be predicted by RANS.model.

***Keywords*—**LES, Mesh, Gas-Solid, Fluidized bed

I. Introduction

THE fluidized bed is one of the most important technologies for heterogeneous gas-solid operations in the petrochemical industry, covering applications in catalytic and non-catalytic processes [2]. The most important industrial applications include catalytic cracking, coal and biomass combustion. One of the most relevant types of fluidized bed reactor is the ascendant flow, which is also known as riser. The fluidized bed consists of a tubular column in which solid and gas flow upwards. The first fluidized bed gas generator was developed in Germany by Fritz Winkler in the 1920s. Later in the 1930s, the American Petroleum Industry Started developing the fluidized bed technology for oil feedstock catalytic cracking, becoming the primary technology for such applications [3]. Applications, advantages and disadvantages to these types of fluidized bed are presented in several publications [4]-[6]. In [7] used LES with discrete particle simulation (DPS) in a vertical turbulent channel flow laden with particles to simulate the experiment of [8].

Large Eddy Simulation was initially applied to the gas flow flowing on solid surface and in atmospheric models [9]-[11] under these circumstances the largest eddies are created away from the solid surface; however the smaller eddies are more visible near the surface.

G. González-Silva is with School of Chemical Engineering, University of Campinas, UNICAMP in Av. Albert Einstein, 500. CEP 13083-970,Campinas-SP, Brazil (germangsilva@feq.unicamp.br)

E. M. Matos is with School of Chemical Engineering, University of Campinas, UNICAMP in Av. Albert Einstein, 500. CEP 13083-970,Campinas-SP, Brazil.

W. P. Martignoniim, Petrobras, RJ, Brazil.

M. Mori is with School of Chemical Engineering, University of Campinas, UNICAMP in Av. Albert Einstein, 500. CEP 13083-970,Campinas-SP, Brazil (mori@feq.unicamp.br)

For this reason it has been recommended to perform a refining mesh near the wall in order to capture small-scale structures. However, for gas-solid flows these small scales appear throughout the control domain. In [12] have reported that the key problem is the selection or construction of the two-phase sub-grid scale (SGS) stress model. In the present work the sub-grid scale turbulence of gas phase is predicited by Smagorinsky´s method and the particle follows the conventional Eulerian method. Results show that it is possible to use mesh with less number of cells as compared to RANS turbulence model with granular kinetic theory flow (KTGF). Also, the numerical results validate the experimental data near wall of the bed, which cannot be predicted by RANS model.

II. Scale Relations

An unstructured mesh with non-uniform grid spacing would normally be used. For the case of a two-phase system, it is recommended to have a refining throughout the control domain; due to the interaction of the two phases that form different turbulent structures (eddies) with different orders of magnitude [13]. A non-uniform mesh with large cell spacing provides an incomplete description of the mesh regarding the resolution of the turbulence and numerical instability. In practice is difficult to generate a mesh size of a refining that is proportional (locally) to the length scale of turbulence [14].

The largest-scale is associated with larger vortices, which also coincides with the characteristic variables of flow velocity (U), length (L) and time (t). The characteristics of these large vortices depend on the flow boundary conditions and present a distinctly anisotropic. The Reynolds number, the frequency and the energy (per unit mass and time) to be dissipated are represented by equations, and respectively.

$$\mathrm{Re} = \frac{UL}{\nu} > 1 \qquad (1)$$

$$f \approx \frac{U}{L} \qquad (2)$$

$$\varepsilon \approx \frac{U^3}{L} \qquad (3)$$

The energy is transferred to intermediate (mesoscales) levels of characteristic velocity (uℓ) and characteristic size ℓ, such that Reℓ>>1, furthermore:

$$\frac{u_\ell}{\ell} \approx \frac{U^3}{L} \rightarrow u_\ell \approx U\left(\frac{\ell}{L}\right)^{\frac{1}{3}} << \mathrm{U} \tag{4}$$

$$f_\ell \approx \frac{u_\ell}{\ell} \approx \frac{U}{L}\left(\frac{L}{\ell}\right)^{\frac{2}{3}} \approx f_L\left(\frac{L}{\ell}\right)^{\frac{2}{3}} >> f_L \tag{5}$$

The small-scales are controlled by the viscosity and they are independent of the large-scale, their motion is isotropic and experience energy dissipation; so that the Reynolds number of small-scales is approximately equal to one.

$$\mathrm{Re}_\eta = \frac{\upsilon\eta}{\nu} \approx 1 \tag{6}$$

According to Kolmogorov, the small-scale turbulence is in equilibrium and controlled only with ε and ν. Kolmogorov defined the length, time and velocity scales of the smallest eddies of the turbulence, as:

$$\eta \equiv \left(\frac{\nu^3}{\ell}\right)^{\frac{1}{4}} \quad , \quad \tau \equiv \left(\frac{\nu}{\varepsilon}\right)^{\frac{1}{2}} \quad , \quad \upsilon \equiv (\nu\varepsilon)^{\frac{1}{4}} \tag{7}$$

Where η is ν kinematic viscosity,

From the filtered continuity and momentum equations follows the relationship between small and large scales of motion, η can be written as

$$\frac{\eta}{L} \approx \mathrm{Re}^{-\frac{3}{4}} \quad , \quad \frac{\upsilon}{U} \approx \mathrm{Re}^{-\frac{1}{4}} \quad , \quad \frac{\tau}{t} \approx \mathrm{Re}^{-\frac{1}{2}} \tag{8}$$

From the dimensions of the fluidized bed domain it is possible to estimate the values of the dimensions of the smallest scales of turbulence. At this point it is necessary to compare the length scales smaller the diameter of the particles. If a particle has a dimension smaller than the smallest Kolmogorov scale, i.e, if the characteristic dimension of particles is smaller than the dissipative scale; the particle only suffers the effects of diffusion. When this particle is a vortex, the trend will follow the path of the vortex and tend to form groups [6], [15]-[17]. In order to determine an appropriate, mesh size (dx) it needs to be proportional to the particle size in the order 8 to 100 particle diameters, because the clusters present in the gas-solid flow have an average diameter of these characteristics [13]-[14], [17]-[21]. When the mesh size is of the order of magnitude of the particle diameter, the simulation can be considered as a direct simulation, even if it is larger than the smallest length scale of turbulence. This notion is of fundamental importance in defining the computational mesh refinement, because the mesh should have such dimensions that do not violate the condition of continuity, i.e, the computational mesh cannot be of the same order of magnitude as the diameter of a particle. Because local media, the equations are not written to capture detailed changes arising from the presence of a single particle, but rather a set of particles. Under this circumstance is only possible to describe the behavior of meso-scales, cluster and strands of fluid dynamics in fluidized beds by applying the Large Eddy Simulation (LES).

III. Mathematical Model

In this paper the transient three-dimensional gas-solid flow is numerically simulated by means of LES for the gas flow and a Eulerian-Eulerian model in which the gas and solid phases are considered as two interpenetrating continuum flows.

A. Continuity Equations

The governing equations are here presented in tensor notation.

$$\frac{\partial}{\partial t}\left(\alpha_g\rho_g\right) + \nabla\cdot\left(\alpha_g\rho_g\vec{v}_g\right) = 0 \tag{9}$$

$$\frac{\partial}{\partial t}\left(\alpha_s\rho_s\right) + \nabla\cdot\left(\alpha_s\rho_s\vec{v}_s\right) = 0 \tag{10}$$

Where α, ρ and are volume fraction, density and the vector velocity for each phase, respectively. The subscripts g and s indicate the gas and particulate phases, respectively. No mass transfer is considered to occur between the phases

B. Momentum Equations

The gas phase momentum equation may be expressed as:

$$\begin{aligned}\frac{\partial}{\partial t}\left(\alpha_g\rho_g\vec{v}_g\right) + \nabla\cdot\left(\alpha_g\rho_g\vec{v}_g\vec{v}_g\right) = \\ -\alpha_g\nabla p + \nabla\cdot\left[\tau_g\right] + \alpha_g\rho_g\vec{g} + \beta\left(\vec{v}_s - \vec{v}_g\right)\end{aligned} \tag{11}$$

p and $\vec{g}$ are fluid pressure and gravity acceleration. β is the drag coefficient between the phases g and s. The stress tensor of phase gas is given by:

$$\tau_g = \alpha_g\mu_g\left[\nabla\vec{v}_g + \left(\nabla\vec{v}_g\right)^T\right] - \frac{2}{3}\alpha_g\mu_g\nabla\vec{v}_g \tag{12}$$

The solid phase momentum equation may be written as:

$$\begin{aligned}\frac{\partial}{\partial t}\left(\alpha_s\rho_s\vec{v}_s\right) + \nabla\cdot\left(\alpha_s\rho_s\vec{v}_s\vec{v}_s\right) = \\ -\alpha_s G\nabla\alpha_s + \nabla\cdot\left[\tau_s\right] + \alpha_s\rho_s\vec{g} + \beta\left(\vec{v}_g - \vec{v}_s\right)\end{aligned} \tag{13}$$

The stress tensor of phase solids is given by:

$$\tau_s = \alpha_s\mu_s\left[\nabla\vec{v}_s + \left(\nabla\vec{v}_s\right)^T\right] - \frac{2}{3}\alpha_s\left[\mu_s\nabla\vec{v}_s\right]\bar{I} \tag{14}$$

Here μ is the shear viscosity, I is the unit tensor and G is the modulus of elasticity given by:

$$G\left(\alpha_s\right) = \exp\left[C_G\left(\alpha_s - \alpha_{s,\max}\right)\right] \tag{15}$$

Where αs,max is the maximum solid volume fraction. For monodispersed spheres, the packing limit is about 0.63. β is the interface momentum transfer proposed by[22]:

$$\alpha_g \le 0.8$$

$$\beta = 150\frac{\alpha_s\left(1-\alpha_g\right)\mu_g}{\alpha_g d_p^2} + 1.75\frac{\alpha_s\rho_g\left|\vec{v}_s - \vec{v}_g\right|}{d_p} \tag{16}$$

$$\alpha_g > 0.8$$

$$\beta = \frac{3}{4}C_D\frac{\alpha_s\alpha_g\rho_g\left|\vec{v}_s - \vec{v}_g\right|}{d_p}\alpha_g^{-2.65} \tag{17}$$

Where d_p and C_D are the particle diameter and the drag coefficient, based in the relative Reynolds number (Res),

$$G(\alpha_s) = \exp\left[C_G\left(\alpha_s - \alpha_{s,\max}\right)\right] \tag{18}$$

$$C_D = \frac{24}{\mathrm{Re}}\left(1 + 0{,}15\,\mathrm{Re}^{0{,}687}\right) \qquad \mathrm{Re}_s < 1000 \tag{19}$$

$$C_D = 0{,}44 \qquad \mathrm{Re}_s \geq 1000 \tag{20}$$

C. Filtered Governing Equations

The LES methodology is a multi-scale fluid dynamics based on the separation of large and small-scale in a turbulent flow. The main operation in large eddy simulation is low-pass filtering. This operation is applied to the Navier-Stokes equations to eliminate small scales of the solution. In LES a filtering operation, is introduced to formally separate the flow to the resolved and unresolved scales. The large scales of motion are simulated directly while the smallest scales - the dissipative scales - are sub-grid part. [23] was the first to use the term Large Eddy Simulation and the idea of filtering as a convolution operation formally on the velocity field, and gave the first general formulation of the method. A filtered variable or large-scale, denoted by an overbar, is defined as

$$\bar{\varphi}(x) = \int_D \varphi(x')\,G\left(x;x';\bar{\Delta}\right)dx' \tag{21}$$

Where D is the fluid domain, G is the filter function that determines the scale of resolved eddies, and is the filter width that determines the size of the largest eddy removed by filtering operation. The unresolved part of the variable φ is defined by

$$\varphi' = \varphi - \bar{\varphi} \tag{22}$$

Contrary to the RANS model in which $\bar{\varphi}' = 0$ the filtered fluctuations in LES are different from zero [24:

$$\bar{\varphi}' \neq 0 \tag{23}$$

The discretization of the domain space in finite control volumes implicitly involves the filtering operation:

$$\bar{\varphi}(x) = \frac{1}{V}\int_V \varphi(x')\,dx' \quad , \quad x' \in V \tag{24}$$

Where V is the volume control. The filter function (called the hat filter or Gaussian filter) is given by:

$$G(x;x') = \begin{cases} 1/V & , \quad x' \in V \\ 0 & , \quad Otherwise \end{cases} \tag{25}$$

D. Subgrid-Scale Models

The filtered equations of Navier-Stokes equations lead to additional unknown variables. The following modeling will be presented to the incompressible equations. The incompressible momentum equation can be written as follows:

$$\frac{\partial \bar{U}_i}{\partial t} + \frac{\partial}{\partial x_j}\left(\bar{U}_i\bar{U}_j\right) = -\frac{1}{\rho}\frac{\partial \bar{p}}{\partial x_i} + \frac{\partial}{\partial x_j}\left[v\left(\frac{\partial \bar{U}_i}{\partial x_j} + \frac{\partial \bar{U}_j}{\partial x_i}\right)\right] - \frac{\partial \tau_{ij}}{\partial x_j} \tag{26}$$

Introducing the sub-grid scale (SGS) stresses, τ_{ij}, as:

$$\tau_{ij} = \overline{U_iU_j} - \bar{U}_i\bar{U}_j \tag{27}$$

The large-scale of turbulent flow is solved directly and the influence of small-scales is taken into account through appropriate sub-grid models. In these simulations, a methodology is used for turbulent viscosity, which relates the SGS τ_{ij} with the rate-of-strain tensor S_{ij}, as follows:

$$-\left(\tau_{ij} - \frac{\delta_{ij}}{3}\tau_{kk}\right) = 2v_{sm}\bar{S}_{ij} \quad , \quad \bar{S}_{ij} = \frac{1}{2}\left(\frac{\partial \bar{U}_i}{\partial x_j} + \frac{\partial \bar{U}_j}{\partial x_i}\right) \tag{28}$$

The difference of RANS models and LES methodology is related to the turbulent viscosity which represents all the turbulent scales and the viscosity sub-grid represents only the smaller scales. The isotropic part is not modelled; however it is added to the static filtered pressure. It was used a sub-grid model for correcting the effective viscosity based on [11]. The Smagorinsky model is an algebraic model that assumes the viscosity as a function of SGS and parameters associated with the cut-off frequency (size of mesh).

$$v_{sm} \propto l\, q_{sm} \tag{29}$$

Where l is the length of scale -usually the size of the mesh, $\Delta = (V)^{1/3}$ - and q_{sm} is the velocity of the unresolved motion. This is based on an analogy to the Prandtl mixing length model, where the velocity scale is related to the gradients of the filtered velocity:

$$v_{sm} = \left(C_S\Delta\right)^2\left|\bar{S}\right| \tag{30}$$

Where Cs is the Smagorinsky constant, nonetheless, a C_s value of around 0.1 has been found to yield the best results for a wide range of flows, and is the default value in ANSYS CFX®. The filter characteristic is computed according to the volume of the computational cell using

$$\Delta = \min\left\{\left(\Delta x, \Delta y, \Delta z\right)^{1/3}, \kappa n\right\} \tag{31}$$

Where κ is The von Karman constant κ, used value of 0.41 and n is the distance to the nearest wall.

The Smagorinsky model eddy viscosity is nonzero at solid boundaries, which is contrary to the notion that the eddy viscosity should be zero where there is no turbulence. To remedy this situation near the walls, the turbulent viscosity can be damped add a Van Driest-style damping function [25] into the length scale f_μ, the resulting equation is:

$$v_{sm} = \min\left(l_{mix}, f_\mu C_S\Delta\right)^2\sqrt{2S_{ij}S_{ij}} \tag{32}$$

With,

$$l_{mix} = \kappa \cdot y_{Wall} \tag{33}$$

$$f_\mu = \sqrt{1 - \exp\left[\left(\frac{y+}{25}\right)^3\right]} \tag{34}$$

$$\oint \rho\phi\vec{v}\cdot d\vec{A} = \rho v_w A_w \phi_W = C_w\phi_W \tag{35}$$

Where C_w is the west face convective coefficient. A_w can be represented by:

$$A_w = MAX(C_w, 0) + D_w \quad (36)$$

IV. Computing Procedure And Results

The data used for validating the CFD model were taken from [1]. The equipment is a laboratory scale fluidized bed with cold-flow solids recirculation unit, located at Norwegian Institute of technology. The riser is made of plexiglass, the column is 1 m high with an internal diameter of 0.032 m. The initial bed height of the catalysts is 0.05 m. The Laser Doppler Anemometry (LDA) is used to measure the radial profiles of the local axial velocity of the particles, at heights 0.16, 0.32 and 0.48 m above the gas distributor. The density of the FCC is 1600 kg/m^3 with a Sauter mean diameter of 55 um.

A. Mesh Parameters and Boundary Conditions

As discussed, η can be expressed as

$$\eta = L\,\mathrm{Re}_1^{-3/4} = 0.36\mu m \quad (37)$$

The size of the smaller-scale is less than the particle size (55μm). This result is used to determine the size of the mesh.

The quality of the mesh is represented by different parameters. The Table I shows the characteristic values of the Jacobian matrix determinant and the minimum internal angle of the element faces of the created mesh.

The superficial gas velocities used in the experiments are 0.36 m/s, 0.71 m/s and 1.42 m/s, respectively at ambient temperature (Table II).

The case studies were carried out by using software CFX® 12.0. The simulations were executed in the transient (dynamic) state. The setting up was done considering the average value of the Courant number (Co) to be near the recommended value of 1. In addition, a constant step time was used in order to improve the numerical stability during the execution of each of the simulations.

TABLE I
Grid Quality Parameters

Parameter	Mesh I	Mesh II
Control volumes number	100,000	500,000
Δ/dx	~ 0.05	~ 0.08
dx/dp	15	10
Determinant of the Jacobian matrix	> 0.5	> 0.5
Minimum angle	> 50°	> 50°

$$Co = \frac{U}{\frac{\min(\Delta x, \Delta y, \Delta z)}{\Delta t}} < 1 \quad (38)$$

$$\Delta t = \frac{Co}{140} \quad (39)$$

Experimental data and LES - Smagorinsky simulations were compared for three velocities with initial particle bed, 5cm and Δt=0.001 s. The boundary conditions for both cases are shown in Table II. Tests were made with a 500.000 control volume mesh with the same block distribution, obtaining similar results with the 100.000 control volume mesh. Both meshes are shown in Fig. 1.

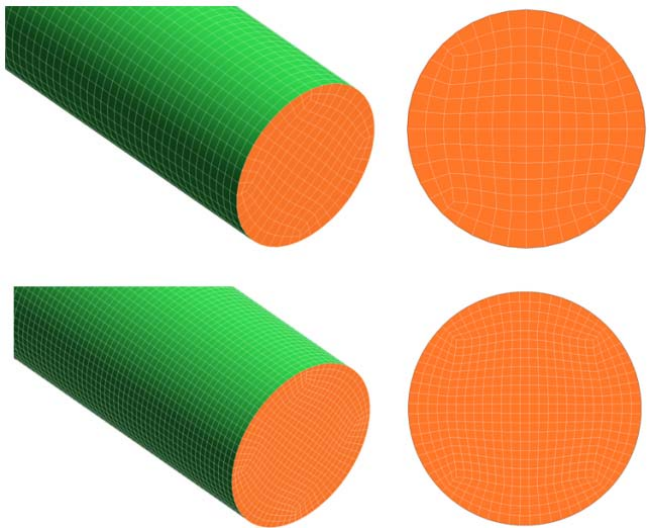

Fig. 1 Schematic diagram of the meshes. Up: Mesh I. Down: Mesh II

Numerical calculations performed by [26]-[27] showed that to obtain an accurate numerical solution it is necessary to use a ratio Δ/dx ≤ 0.25 for the second order spatial scheme, and a ratio Δ/dx < 0.5 for the sixth order scheme.

The values of Δ/dx presented in Table I are within the range recommended in the literature [13], [17]-[18], [26]-[27].

Fig. 2 shows the solid velocity profiles for the three heights for the superficial gas velocities of 1.42 m s^{-1}, 071 m s^{-1} and 0.36 m s^{-1}.

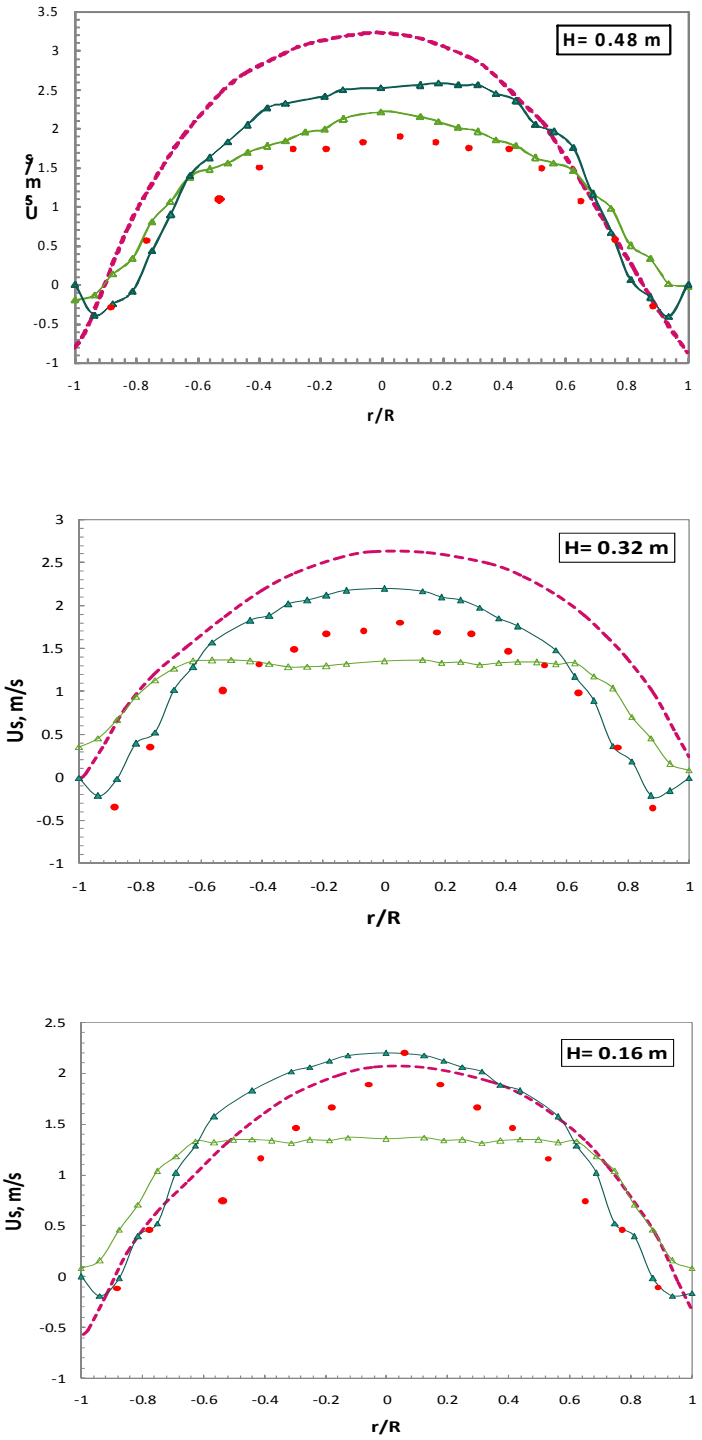

Fig. 2 Radial profiles of particle velocity along the riser different operating conditions, U_g=1.42 m/s. ● Experimental; --- [28]; -▲- No Slip; -Δ- Free slip

TABLE II
BOUNDARY CONDITIONS

In	Gas velocity = 0.36;0.71, 1.42 m/s Particle mass flow equal to the output
Out	Opening = atmospheric pressure
Wall	Particles = free slip and No slip Gas = no slip
Initial height	Bed height = 0,05 m
Particles	60 µm; 1600 kg/m3

Exist similarity between the results presented by [29] , the regions of high and low solids volume fraction are well represented by the mathematical model. Simulations by [28] were conducted in a com geometry approximately 280,000 control volumes using RMS with granular kinetic theory. Each simulation required about two months to simulate 15 seconds of real time

It can be observed in Table III that CPU time was significantly reduced in comparison to the data reported by [28].

Also, the number of control volumes was decreased by a factor of three using the quasi-uniform mesh discretization. Fig.3 shows the core-annulus behavior in more detail. High concentrations of solids in the region near the wall and low concentrations in the center are observed in the cross-sections for the three heights analyzed.

TABLE III
COMPARISON OF THIS WORK AND THE DATA REPORTED BY HODAPP [28] IN TERMS OF CPU TIME AND NUMBER OF CONTROL VOLUMES

	Δt (s)	Real time (s)	CPU Time (Day)	Control Volumes	Processor	Core/Memory
[28]	0,001	15	60	278000	2,4 GHz	6/1GB
This work	0,001	15	12-18	100000	1.6 GHz	6/4GB

With the implementation of the LES to the gas phase, it was possible to identify the core-annulus flow, characteristic of fluidized beds, which the [30], the behavior of core-annulus may increase the inefficiency of the gas-solid contact.

The phenomenon of core-annulus and radial diffusion of particles to the wall is believed to occur due to concentration gradients in the dilute phase, forming accumulations or clusters of particles near the walls.

Thus, the phenomenon of cluster prevails along the main line of core-annulus. The overestimation of the velocities of the particle may be due to the fact that the electrostatic forces present in the experiments were not incorporated into the model, also because of the error that causes the kind of experimental technique used.

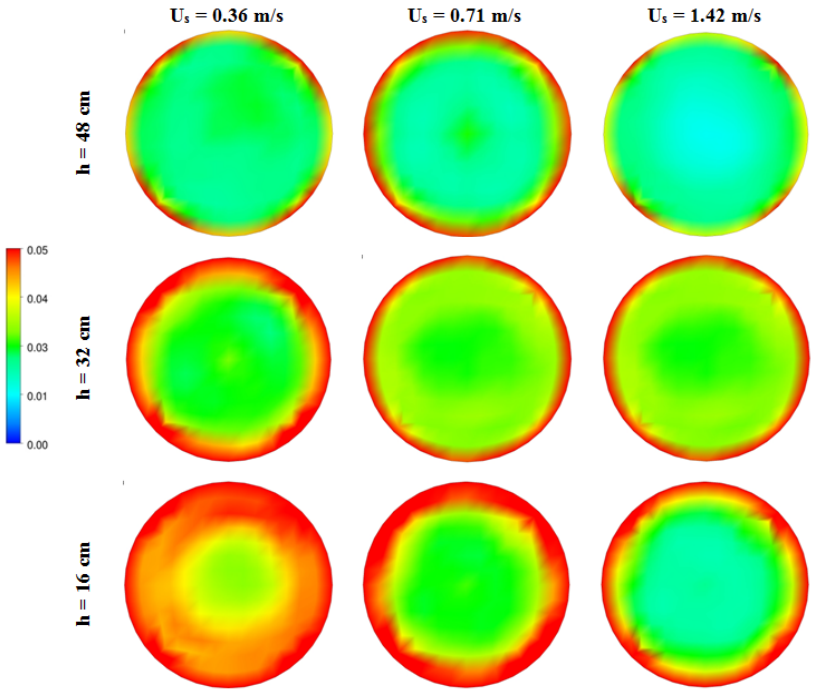

Fig. 1 Cross-section profiles of solids volume Fraction

No-slip condition increases the accumulation of particles near the walls. Some authors say that the condition on the wall does not influence the final results of the simulation [13], [19]; however it is clear that both conditions show different behaviors in the center and in the wall of riser for the three gas superficial velocities, as shown in Fig. 4.

An important question is to define at what level of scale should be simulated gas-solid system, to be applied industrially. In industrial reactors over 30 meters high, the definition of a mesh size suitable for describing the behavior of certain scales, as for example mesoscale, it is very important for predicting and minimizing experimental costs.

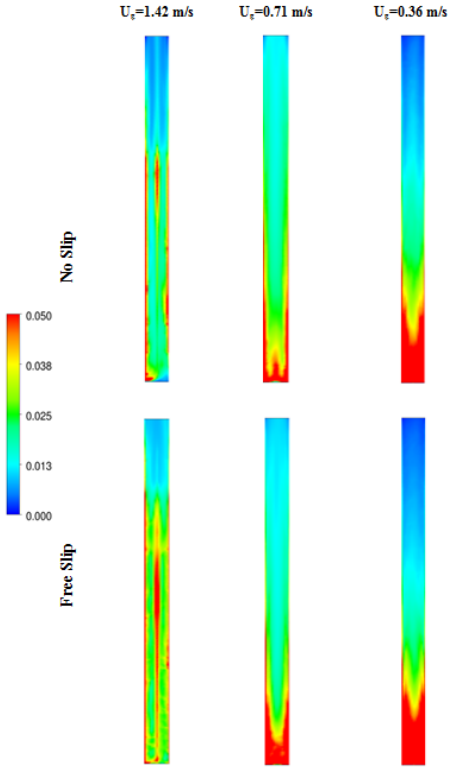

Fig. 4 Volume fraction of solid in the center of the riser (XY plane): Free slip (top) and No-Slip (bottom) for solids.

The importance of this work is in the implementation of the LES methodology for gas-solid flows, using a coarse mesh with quasi-uniform cells. The sub-grid models along with uniform coarse-grid can capture the radial solid velocity profile near the fluidized bed wall, which is not possible by means of other turbulent models such as RANS and RMS with granular kinetic theory. The numerical simulation was compared with experimental data by [1] .in fluidized beds. Predicitons are also compared with simulate data reported by [28].

A maximum Co number of 0.5 gives adequate numerical stability and temporal accuracy, however a value of Co ≈ 0.2 is preferable since LES attempts to resolve and capture the dynamics of resolvable eddies and large coherent structures.

When advection dominates dispersion, a model with a small Courant number (Co < 1) will decrease oscillations, improve accuracy and decrease numerical dispersion. Lower Courant number (0 > Co ≥ 0.5) means better stability but slower calculation, higher Courant number (1 ≥ Co ≥ 0.5) is just the contrary . But this subject is controversial and should not be generalized, depending on the problem to be analyzed (geometry, boundary conditions, mesh, etc.).

Fig. 2 shows the mean values of Courant number is less than one, regardless of the wall condition for the three superficial gas velocities. Also seen that the values of Courant number are small near the wall and higher in the center, consistent with the velocity fields.

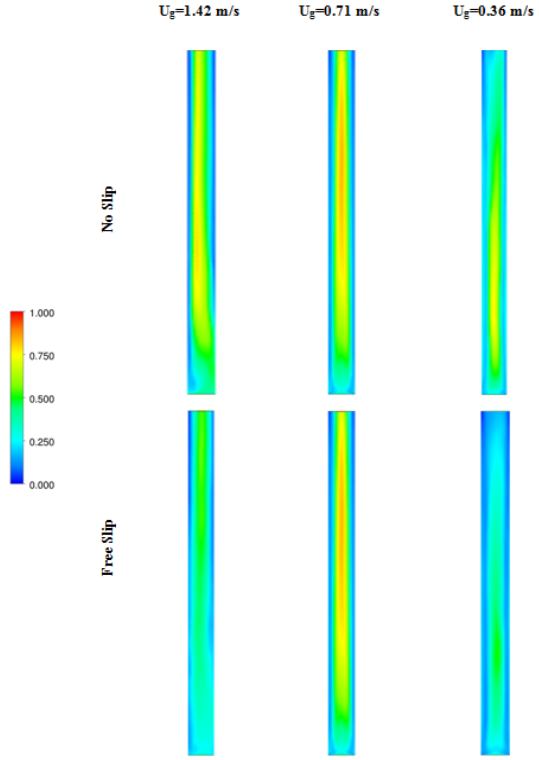

Fig 1 Average Courant Number at the center of the riser (XY plane): Free slip (top) and No-Slip (bottom).

V. Conclusions

The LES approach in this work using quasi-uniform meshes has implemented to minimize the computational effort and procedure for refining the mesh. As a consequence of using meshes of uniform size reduced enormously the computational effort. For the gas-solid phases it was noticed that no need for refinement near the walls of the fluidized bed as reported by [31]-[34. By using non-uniform meshes in LES methodology produce numerical instability. However, a careful examination for mesh generation is necessary in order to have an uniform control volumes. The no-slip condition for the gas-solid system was the best initial condition which can capture the behavior of the system near the wall. Although the simulation results with the free-slip condition showed similar profiles.

By applying LES approach it was possible to describe the characteristics of different regions of a fluidized bed as the core-annulus. Results of this work indicate that CPU time was significantly reduced in comparison to the results predicted by RANS model. Also, the number of control volumes was decreased by a factor of three using the quasi-uniform mesh configurations.

In conclusion, in the case of gas-solid flow, it is imperative to calculate the values of the sub-scales of space and time from the relations between micro and macro scales throughout the entire domain and not only near the walls.

ACKNOWLEDGMENT

The author G. S Gonzalez is grateful to PETROBRAS and the National Council for Scientific and Technological Development (CNPq) for the financial support to this research.

REFERENCES

[1] .A. Samuelsberg, and B. H. Hjertager, "An experimental and numerical study of flow patterns in a circulating fluidized bed reactor." International Journal of Multiphase Flow 22 (3) (June): 575-591, 1996.

[2] D. Kunii, and O. Levenspiel, "*Fluidization engineering".* 2nd ed. Boston Mass.: Butterworth-Heinemann, 1991

[3] E S. Tavoulareas, "Fluidized-Bed Combustion Technology." Annual Review of Energy and the Environment 16 (1) (November): 25-57. 1991.

[4] J. Ancheyta, "Modeling and simulation of catalytic reactors for petroleum refining". Oxford: Wiley-Blackwell, 2010.

[5] G. S. Gonzalez,, 2008. "*Modeling and simulation of cocurrent downflow reactor (Downer*)". Master's thesis, Campinas, Brazil: University of Campinas.

[6] Y. Cheng, W. Changning, Z. Jingxu, Fei Wei, and Yong Jin. "Downer reactor: From fundamental study to industrial application." *Powder Technology* 183 (3) (April 21), 2008.

[7] J. K. Eaton and J. R. Fessler. Preferential concentration of particles by turbulence. International Journal of Multiphase Flow, 20(Supplement 1):169–209, August 1994.

[8] Kulick Jd, Fessler Jr, and Eaton Jk. Title: particle response and turbulence modification in fully-developed channel flow author(s): kulick jd, fessler jr, eaton jk source: journal of fluid mechanics 277: 109-134 oct 25 1994. *journal of fluid mechanics*, 277:109–134, 1994

[9] J.W. Deardorff, "Three-dimensional numerical study of the height and mean structure of a heated planetary boundary layer." *Boundary-Layer Meteorology* 7 (1) (August), 1974.

[10] DK Lilly,. The representation of small scale turbulence in numerical simulation experiments. In *IBM Scientific Computing Symposium on environmental sciences*, 195-210, 1967.

[11] J. Smagorinsky. "General circulation experiments with the primitive equations". Monthly Weather Review, 91(3):99–164, March 1963.

[12] Liu Han-Tao,Chang Jian-Zhong,An Kang et al. "Direct numerical simulation of the sedimentation of two particles with thermal convection". *Acta Phys. Sin*., 2010, 59(3): 1883-1883.

[13] K. Agrawal, P N. Loezos, M Syamlal, and S Sundaresan. "The role of meso-scale structures in rapid gas-solid flows". Journal of Fluid Mechanics, 445:–185.

[14] I. C. Georg,. "*Modelagem e simulação numérica tridimensional transiente do escoamento gás-sólido em um reator de craqueamento catalítico em leito fluidizado*" PhD diss., Florianópolis: Universidade Federal de Santa Catarina. 2005.

[15] CY Yang, and U Lei. "The role of the turbulent scales in the settling velocity of heavy particles in homogeneous isotropic turbulence." J. *Fluid Mech.* 371: 179-205, 1998.

[16] J. R Fessler, and John K. Eaton. "Turbulence modification by particles in a backward-facing step flow." *Journal of Fluid Mechanics* 394 (September): 97-117. 1999.

[17] A. M., Ahmed, and S. Elghobashi "On the mechanisms of modifying the structure of turbulent homogeneous shear flows by dispersed particles." *Physics of Fluids* 12: 2906, 2000.

[18] van Wachem B.G.M.. *Derivation, Implementation, and Validation of Computer Simulation Models for Gas-Solid Fluidized Beds.* Ph.D. Thesis, Delft University of Technology, 2000

[19] P N Andrews,. Loezos, and Sankaran Sundaresan. "Coarse-Grid Simulation of Gas-Particle Flows in Vertical Risers." *Industrial & Engineering Chemistry Research* 44 (16): 6022-6037. 2005.

[20] Y. A. Igci, S Sundaresan, S Pannala, and T O'Brien. "Filtered two-fluid models for fluidized gas-particle suspensions." *AIChE Journal* 54 (6): 1431-1448. 2008.

[21] W. Holloway, B Sofiane, Christine M. Hrenya, and Sankaran Sundaresan. 2011. "Meso-scale structures of bidisperse mixtures of particles fluidized by a gas." Chemical Engineering Science 66 (19) (October 1): 4403-4420.

[22] D. GeldartGas, "*Fluidization technology"*. Chichester, New York: Wiley, 1986.

[23] A. Leonard. Energy cascade in large-eddy simulations of turbulent fluid flows. In Turbulent diffusion in environmental pollution; Proceedings of the Second Symposium, Charlottesville, Va., April 8-14, 1973. Volume A. (A75-30951 13-47) New York, Academic Press, Inc., 1974, p. 237-248. NASA-supported research., volume 75, pages 237–248, 1974.

[24] S., Ghosal, and P. Moin, "The Basic Equations for the Large Eddy Simulation of Turbulent Flows in Complex Geometry." *Journal of Computational Physics* 118 (1) (April): 24-37, 1995

[25] van Driest, E. R. "On the turbulent flow near a wall." *J. Aero. Sci*. 23: 1007-1011, 1956

[26] B. Vreman, B. Geurts, and J. G. M. Kuerten. 'Large-eddy simulation of the turbulent mixing layer'. *J. Fluid Mech*., 339:357–390, 1997.

[27] F. K. Chow and P. Moin, "A further study of numerical errors in large-eddy simulations," *Journal of Computational Physics*, vol. 184, no. 2, pp. 366–380, 2003

[28] Hodapp. "Modeling and simulation of a fluidized bed : a comparative study". Master's thesis, Campinas, Brazil: University of Campinas, 2009.

[29] A. Miller, Aubre, and D. Gidaspow, "Dense, vertical gas-solid flow in a pipe." *AIChE Journal* 38 (11): 1801-1815, 1992.

[30] L. Huilin and D. Gidaspow, "Hydrodynamics of binary fluidization in a riser: CFD simulation using two granular temperatures", Chemical Engineering Science, n.58, p.3777-3792, 2003.

[31] M. Rudman and H. M. Blackburn, Large eddy simulation of turbulent pipe flow. *2 International Conference on CFD in the Minerals and Process Industries, CSIRO*, Melborne, Australia 6−8, 503, 1999

[32] U. Plomelli, "Wall layer models for LES". *46th AIAA Aerospace Sciences Meeting and Exhibit* 7 - 10 January 2008, Reno, Nevada

[33] U. Piomelli, and J. Liu, "Large-eddy simulation of rotating channel flow using a localized dynamic model". *Phys. Fluids* 7, 839-848, 1995.

[34] U. Piomelli, A.,Scotti, E. Balaras, Large-eddy simulation of turbulent flows from desktop to supercomputer, *Proceeding of the Fourth International Conference on Vector and Parallel Processing* vol. 3, Springer (2000).